

# Formation Mechanisms and Edible Applications of Molecular Compound (MC) Forming Mixture Systems of Saturated-Unsaturated Mixed-Acid Triacylglycerols

Ken Taguchi<sup>1</sup>, Laura Bayes-Garcia<sup>2</sup>, Kiyotaka Sato<sup>1</sup>, Lu Zhang<sup>3</sup>, Shinichi Yoshikawa<sup>4</sup>, F Kaneko<sup>5</sup>, Yoshinori Yamamoto<sup>6</sup>, and Shimpei Watanabe<sup>4</sup>

<sup>1</sup>Hiroshima University

<sup>2</sup>Universitat de Barcelona

<sup>3</sup>Affiliation not available

<sup>4</sup>Fuji Oil Holdings Inc.

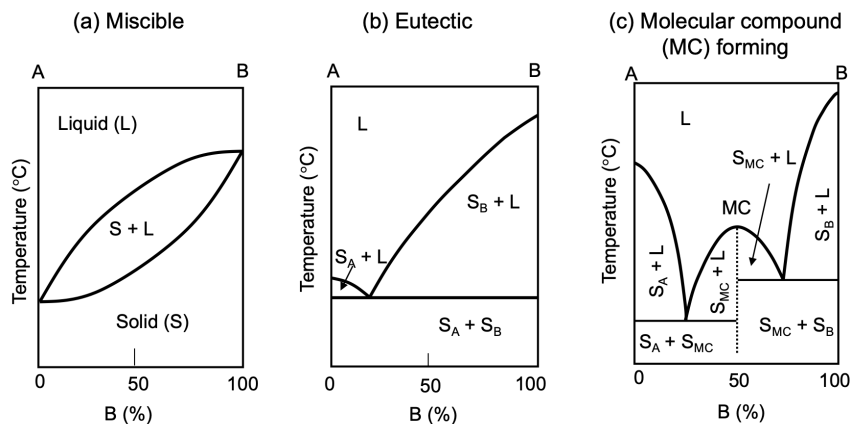
<sup>5</sup>Osaka University

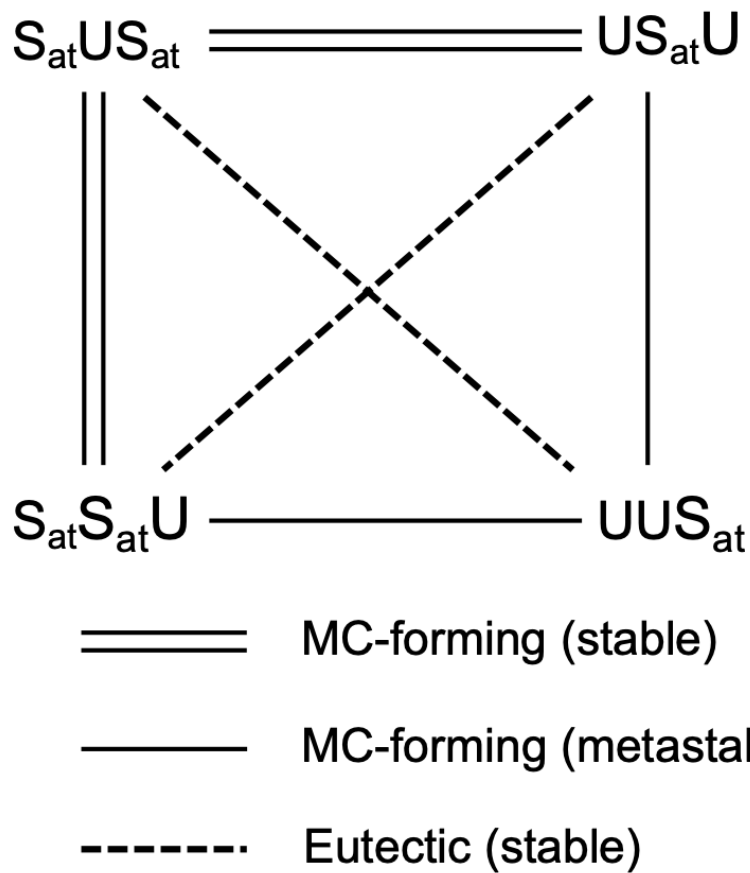
<sup>6</sup>Osaka Daigaku

August 4, 2023

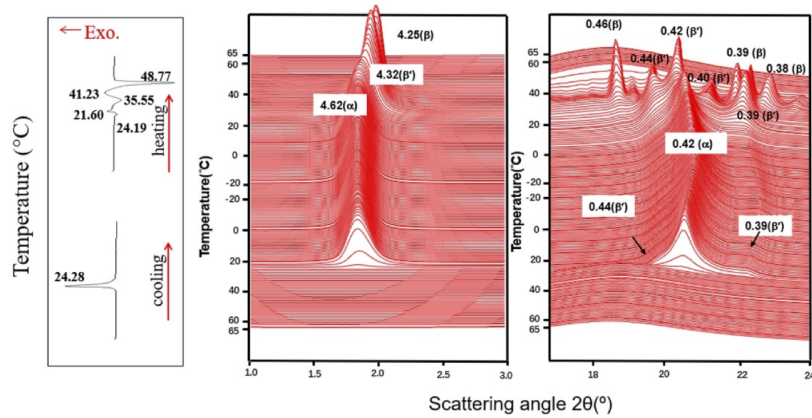
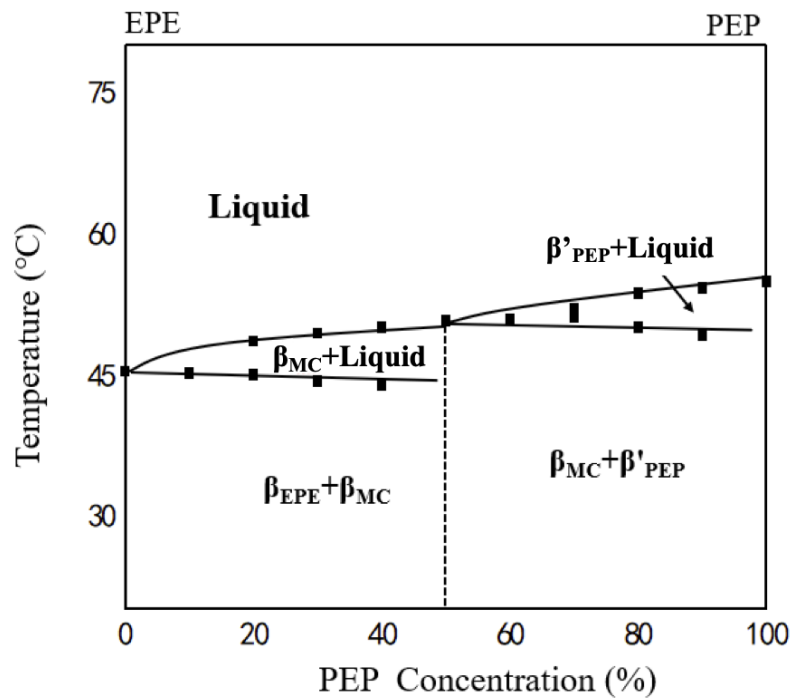
## Abstract

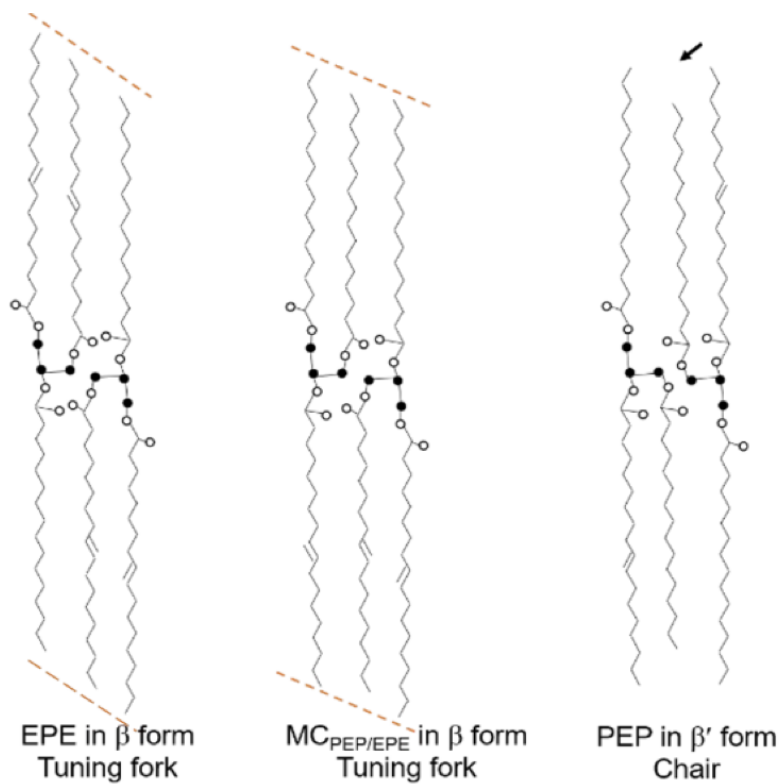
The triacylglycerols (TAGs) containing saturated (Sat) -unsaturated (U) fatty acid moieties (Sat-U mixed acid TAGs) are widely present in most natural fats and employed in many industrial applications. The mixing behavior of different Sat-U mixed acid TAGs acts important roles in the physicochemical properties TAG-based materials. Among the three main mixing states of miscible, eutectic and molecular compound (MC) forming mixtures, fundamental research has been conducted on the MC crystals formed by different Sat-U mixed acid TAGs to understand the structures, phase behavior and crystallization properties. This article reviews recent studies on the complex thermodynamic, kinetic and structural factors that affect the formation of MC crystals in binary and ternary mixtures of Sat-U mixed acid TAGs (SatUSat, SatSatU, USatU and UUSat) through specific molecular interactions among the component TAGs. Furthermore, the application of the MC-forming mixtures containing cacao butter to new types of cocoa butter alternative is reviewed.



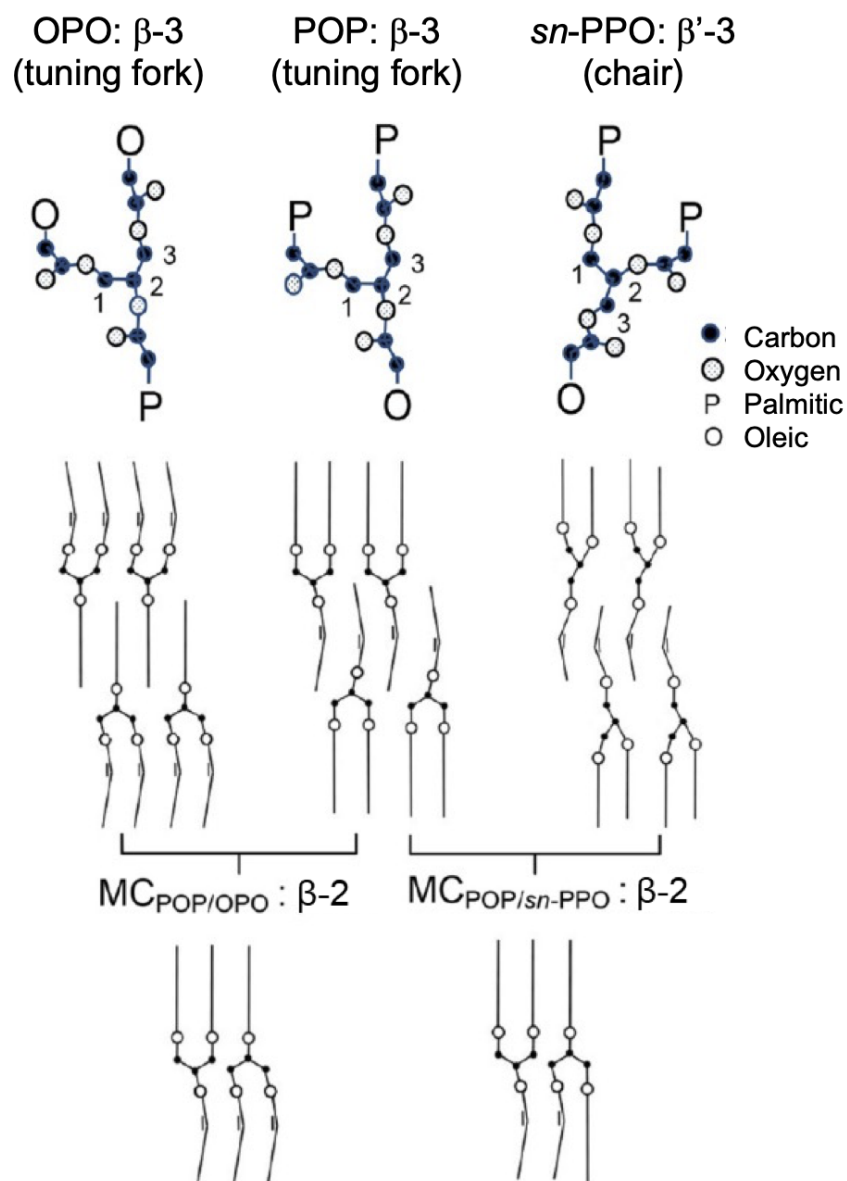


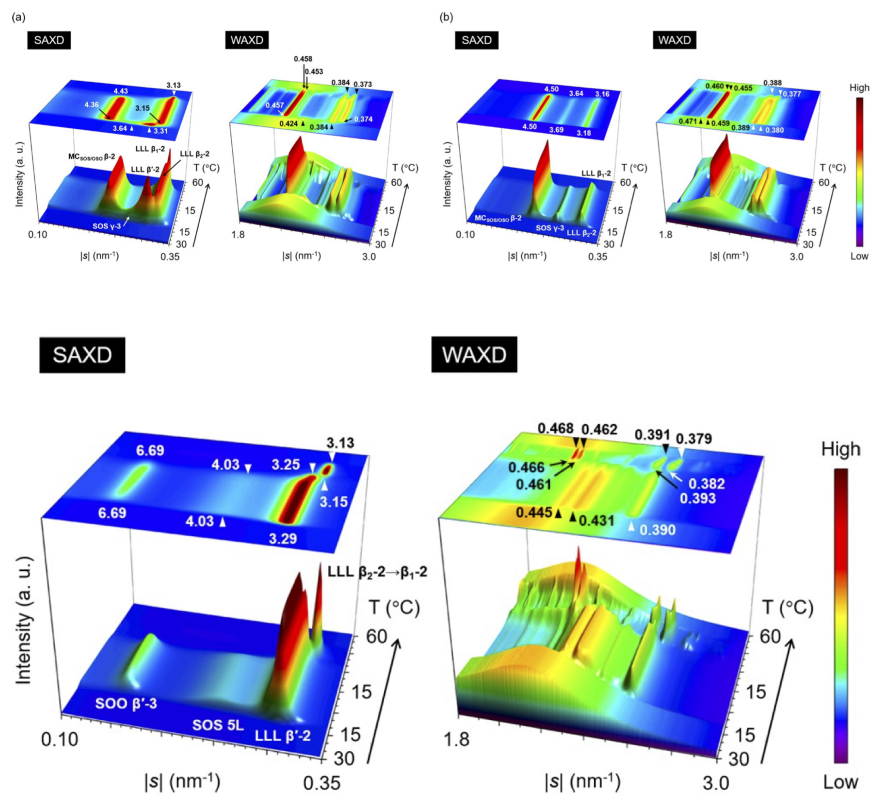
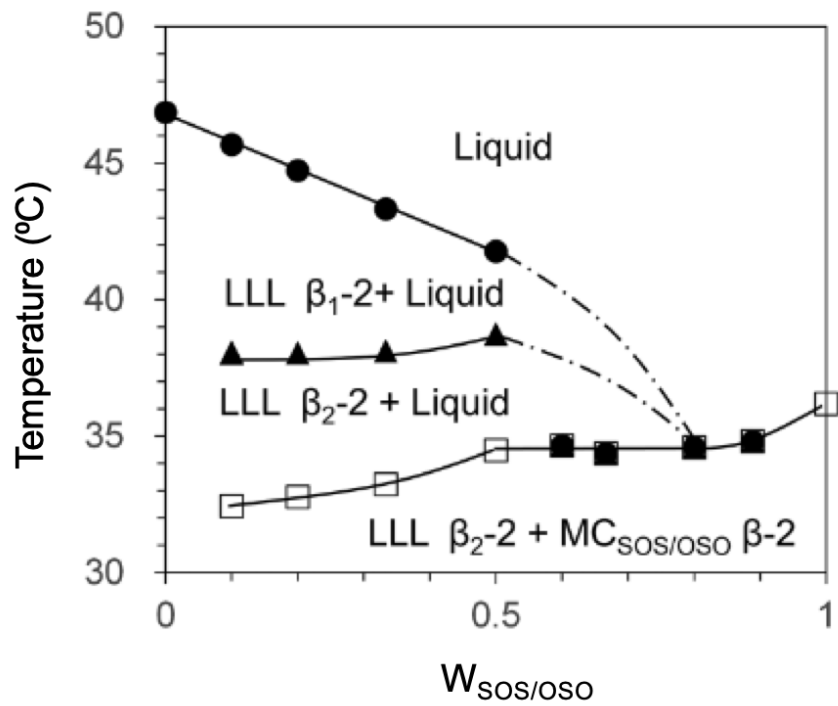
Glycerol conformation				Structural models of MC crystal					
Tuning fork		Chair		POP/OPO	POP/PPO	POP/OOP			
POP	OPO	PPO	OOP			case 1	case 2		
				OPO/OOP	PPO/OOP	PPO/OOP			
						case 1	case 2		

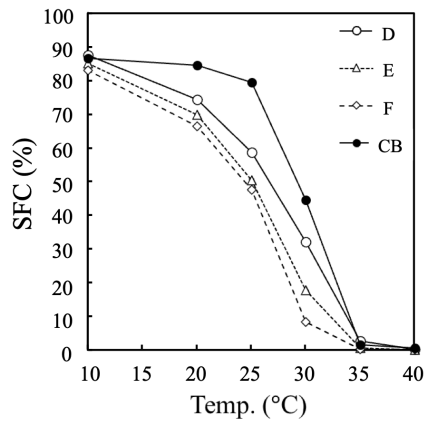
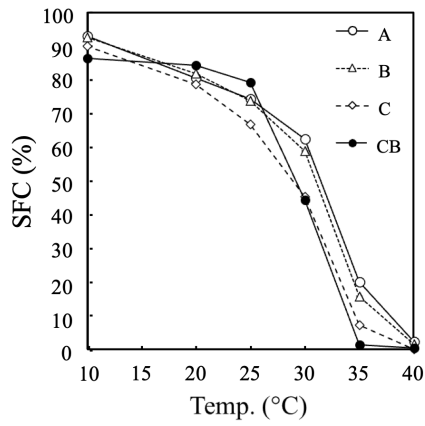
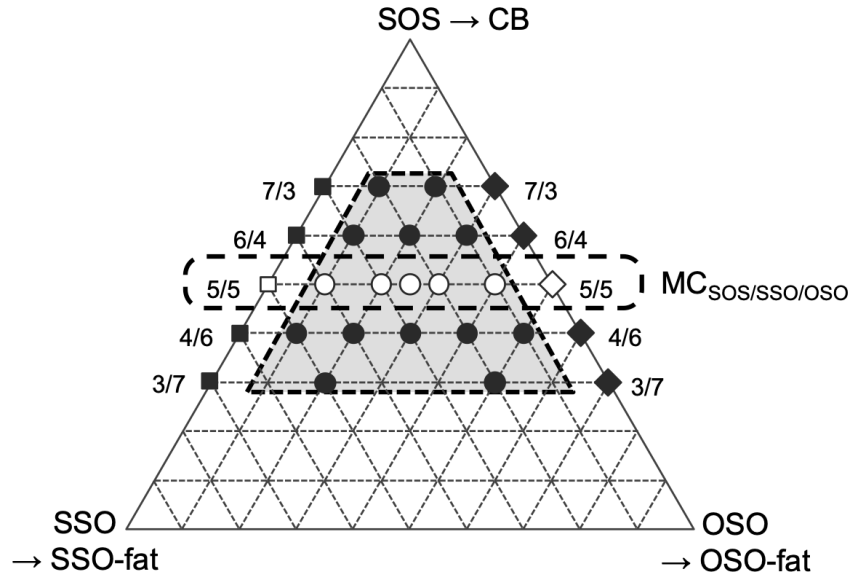




Cooling	Heating (2 °C/min)
<b>POP/OPO</b>	
L $\xrightarrow{0.1; 0.5; 2\text{ °C/min}}$ $\beta$ -2 ( $MC_{POP/OPO}$ )	—————→ L
<b>POP/rac-PPO</b>	
L $\xrightarrow{0.1\text{ °C/min}}$ $\beta$ -2 ( $MC_{POP/rac-PPO}$ )	—————→ L
L $\xrightarrow{0.5; 2\text{ °C/min}}$ $\beta'$ -2 ( $MC_{POP/rac-PPO}$ )	—————→ L → $\beta$ -2 ( $MC_{POP/rac-PPO}$ ) → L
<b>POP/sn-PPO</b>	
L $\xrightarrow{0.1; 0.5\text{ °C/min}}$	$\beta'$ -3 ( <i>sn</i> -PPO) —————→ L
	$\beta'$ -2 ( $MC_{POP/sn-PPO}$ ) —————→ L → $\beta$ -2 ( $MC_{POP/sn-PPO}$ ) → L
	$\beta'$ -2 (POP) —————→ L
L $\xrightarrow{2\text{ °C/min}}$	$\beta'$ -3 ( <i>sn</i> -PPO) —————→ L
	$\alpha$ -2 ( $MC_{POP/sn-PPO}$ ) → L → $\beta'$ -2 ( $MC_{POP/sn-PPO}$ ) → $\beta$ -2 ( $MC_{POP/sn-PPO}$ ) → L
	$\alpha$ -2 (POP) —————→ L → $\beta'$ -2 (POP) —————→ L
$\alpha$ -2 ( <i>sn</i> -PPO) —————→ L	







1           **Formation Mechanisms and Edible Applications of Molecular**  
2           **Compound (MC) Forming Mixture Systems of Saturated-Unsaturated**  
3           **Mixed-Acid Triacylglycerols**  
4

5           Laura Bayés-García<sup>1</sup>, Kiyotaka Sato<sup>2</sup>, Lu Zhang<sup>3</sup>, Shinichi Yoshikawa<sup>4</sup>, Fumitoshi Kaneko<sup>5</sup>,  
6           Yoshinori Yamamoto<sup>6</sup>, Shimpei Watanabe<sup>7</sup>, Ken Taguchi<sup>8</sup>

7  
8           <sup>1</sup>Laura Bayés-García: Departament de Mineralogia, Petrologia i Geologia Aplicada, Facultat de  
9           Ciències de la Terra, Universitat de Barcelona, Martí i Franquès s/n, E-08028 Barcelona, Spain,  
10          [laurabayes@ub.edu](mailto:laurabayes@ub.edu) [orcid.org/0000-0003-1481-581X](https://orcid.org/0000-0003-1481-581X)

11          <sup>2</sup>Kiyotaka Sato: Faculty of Applied Biological Science, Hiroshima University, Higashi-Hiroshima  
12          739-8528, Japan, [kyosato@hiroshima-u.ac.jp](mailto:kyosato@hiroshima-u.ac.jp)

13          <sup>3</sup>Lu Zhang: College of Food and Bioengineering, University of Light Industry, Zhengzhou, China,  
14          [lulu@zzuli.edu.cn](mailto:lulu@zzuli.edu.cn), [orcid.org/0000-0002-8902-0520](https://orcid.org/0000-0002-8902-0520)

15          <sup>4</sup>Shinichi Yoshikawa: Research Institute for Creating the Future, Fuji Oil Holdings Inc., Izumisano  
16          598-8540, Japan, [yoshikawa.shinichi@so.fujioil.co.jp](mailto:yoshikawa.shinichi@so.fujioil.co.jp) [orcid.org/0000-0003-1224-8743](https://orcid.org/0000-0003-1224-8743)

17          <sup>5</sup>Fumitoshi Kaneko: Graduate School of Science, Osaka University, Toyonaka 560-0043, Japan,  
18          [toshi@chem.sci.osaka-u.ac.jp](mailto:toshi@chem.sci.osaka-u.ac.jp) [orcid.org/0000-0001-8254-2265](https://orcid.org/0000-0001-8254-2265)

19          <sup>6</sup>Yoshinori Yamamoto: Graduate School of Science, Osaka University, Toyonaka 560-0043, Japan,  
20          [yamamotoy16@chem.sci.osaka-u.ac.jp](mailto:yamamotoy16@chem.sci.osaka-u.ac.jp)

21          <sup>7</sup>Shimpei Watanabe: Research Institute for Creating the Future, Fuji Oil Holdings Inc., Tsukubamirai  
22          300-2497, Japan, [watanabe.shimpei@so.fujioil.co.jp](mailto:watanabe.shimpei@so.fujioil.co.jp) [orcid.org/0000-0002-9040-3887](https://orcid.org/0000-0002-9040-3887)

23          <sup>8</sup>Ken Taguchi: Graduate School of Advanced Science and Engineering, Hiroshima University,  
24          Higashi-Hiroshima 739-8521, Japan, [ktaguchi@hiroshima-u.ac.jp](mailto:ktaguchi@hiroshima-u.ac.jp) [orcid.org/0000-0003-1276-0499](https://orcid.org/0000-0003-1276-0499)

25

26 **Keywords** Triacylglycerols, Mixing behavior, Molecular compound crystal, Cocoa butter  
27 equivalent, Cocoa butter substitute

28

## 29 **Abstract**

30 The triacylglycerols (TAGs) containing saturated ( $S_{at}$ ) -unsaturated (U) fatty acid moieties (Sat-U  
31 mixed acid TAGs) are widely present in most natural fats and employed in many industrial applications.  
32 The mixing behavior of different Sat-U mixed acid TAGs acts important roles in the physicochemical  
33 properties TAG-based materials. Among the three main mixing states of miscible, eutectic and  
34 molecular compound (MC) forming mixtures, fundamental research has been conducted on the MC  
35 crystals formed by different Sat-U mixed acid TAGs to understand the structures, phase behavior and  
36 crystallization properties. This article reviews recent studies on the complex thermodynamic, kinetic  
37 and structural factors that affect the formation of MC crystals in binary and ternary mixtures of Sat-U  
38 mixed acid TAGs ( $S_{at}U_{Sat}$ ,  $S_{at}S_{at}U$ ,  $U_{Sat}U$  and  $UU_{Sat}$ ) through specific molecular interactions among  
39 the component TAGs. Furthermore, the application of the MC-forming mixtures containing cacao  
40 butter to new types of cocoa butter alternative is reviewed.

## 41 INTRODUCTION

42 The physicochemical properties (e.g., texture, rheology, melting behavior, spreadability,  
43 appearance, *etc.*) of lipid-based products in the food, pharmaceutical and cosmetic industries are  
44 largely determined by the polymorphic and mixing behavior of the constituent triacylglycerols (TAGs)  
45 (Larsson et al., 2006, Floeter et al., 2018).

46 The polymorphic crystallization of TAGs, often based on complex simultaneous processes, and  
47 the phase transformation phenomena are determined by many different factors, such as the chemical  
48 nature of the fatty acid moieties in the TAG structures, and the crystallization conditions applied, which  
49 can be tailored in many different ways by the application of external factors (Bayés-García et al.,  
50 2015a), such as the use of dynamic thermal treatments (Bayés-García et al., 2013; Bayés-García et al.,  
51 2016; Bayés-García et al., 2018), sonication (Martini, 2013; Chen et al., 2013; Ye et al., 2014; Lee et  
52 al., 2015), shear (Sonwai et al., 2006; Mazzanti et al., 2011; Acevedo et al., 2012; Acevedo et al.,  
53 2014), emulsification (Povey et al., 2014; Douaire et al., 2014), additives (Smith et al., 2011;  
54 Yoshikawa et al., 2014; Bayés-García et al., 2022)). An in-depth understanding of the polymorphism  
55 and mixing behavior of TAG components in binary, ternary and even more complex systems is then  
56 required for the optimal control and design of industrial lipid crystallization procedures.

57 The mixing behavior of TAGs has been comprehensively reviewed by several authors (Floeter  
58 et al., 2018; Zhang et al., 2018; Macridachis et al., 2020). Among all TAG species, those with  
59 saturated-unsaturated mixed-acid compositions are widely present in most natural fats and used in  
60 industrial applications. Therefore, extensive research has been carried out in their binary (Koyano et  
61 al., 1992; Minato et al., 1997a; Minato et al., 1997b; Rousset et al., 1998; Takeuchi et al., 2002; Zhang  
62 et al., 2007; Zhang et al., 2009; Ikeda et al., 2010; Mizobe et al., 2013; Ikeda et al., 2014; Bayés-García  
63 et al., 2015b; Nakanishi et al., 2018; Cholakova et al., 2023; Alishevich et al., 2023; Wijarnprecha et  
64 al., 2023), ternary (Koyano et al., 1993; Sasaki et al., 2012; Watanabe et al., 2018; Ghazani et al.,  
65 2019a; Macridachis et al., 2021; Macridachis et al., 2022; Yoshikawa et al., 2022) and multicomponent

66 mixture systems (Bayés-García et al., 2017; Watanabe et al., 2021a). In parallel with the experimental  
67 studies on the TAG mixtures, theoretical studies have been carried out to model and predict the mixing  
68 behavior of different TAGs (Wesdorp et al., 2013; Seilert et al., 2021).

69 Although the number of molecules involved in complex end products is often on the order of  
70 several hundred (Myher et al., 1988; Gresti et al., 1993), the study on the solid-state miscibility on a  
71 smaller scale with a reduced number of TAG components, usually through binary or ternary mixtures,  
72 has been shown to provide highly valuable information that can be extrapolated to real fats, such as  
73 extra virgin olive oil (Bayés-García et al., 2017), cocoa butter (Sasaki et al., 2012; Ghazani et al.,  
74 2019a; Ghazani et al., 2019b), cocoa butter and coconut oil (Joshi et al., 2020), palm oil (Gibon et al.,  
75 1996; Minato et al., 1996; Minato et al., 1997a; Lu et al., 2019; Gibon & Danthine, 2020), milk fat/palm  
76 oil/palm stearin mixtures (Mao et al., 2023) .

77 There are three main mixed states resulting from molecular interactions in binary systems of  
78 TAGs. In a miscible mixture (Figure 1a), a solid solution is formed at all the mixing ratios between  
79 the component TAGs with similar thermal stability and a high degree of isopolymorphism, as the  
80 integration of one crystal phase into the other does not cause any significant disturbance in crystal  
81 packing (Lusi, 2018). By contrast, dissimilar TAG components lead to eutectic behavior as shown in  
82 Figure 1b, where the eutectic composition and the degree of partial solid miscibility can be determined  
83 by, among other things, chain-length structures and melting behavior (Timms, 1984; Minato et al.,  
84 1996; Floeter et al., 2018; Cholakova, 2023).

85 Of particular interest is the third mixed state of the molecular compound (MC) formation (Figure  
86 1c). This stoichiometric compound is formed only at well-defined compositions by specific molecular  
87 interactions between individual TAGs, resulting in unique structural and thermodynamic properties  
88 (see below). The wide range of possibilities given by chemical nature and processing conditions of the  
89 component TAGs may be further enhanced by the use of MC products due to their applicability in  
90 edible fat structuring. For example, the potential of MC crystals as partial replacers for *trans* or

91 saturated fats has already been demonstrated by increasing melting temperature, hardness and solid fat  
92 content (Mykhaylyk et al., 2007).

93 In this review, a special emphasis has been given to the crucial role and potential applicability  
94 of MC-forming mixture systems to modify of the physicochemical properties of lipid structures. It  
95 should be noted that complex thermodynamic, kinetic and structural factors largely affect the  
96 formation of MC in saturated-unsaturated-saturated ( $S_{at}US_{at}$ )/ $US_{at}U$  and  $S_{at}US_{at}/S_{at}S_{at}U$  systems  
97 through specific molecular interactions among the component TAGs.

98 As a fundamental study to elucidate the formation mechanisms of MC, precise observation was  
99 performed on the crystallization behavior of palmitic-oleic-based MC of 1,3-dipalmitoyl-2-oleoyl-  
100 glycerol (POP)/1,3-dioleoyl-2-palmitoyl glycerol (OPO), POP/1,2-dipalmitoyl-3-oleoyl-*rac*-glycerol  
101 (*rac*-PPO) and POP/1,2-dipalmitoyl-3-oleoyl-*sn*-glycerol (*sn*-PPO) when subjected to varied cooling  
102 rates. By comparing the crystallization behavior of POP/*sn*-PPO and POP/*rac*-PPO systems, the effects  
103 of glycerol structures and optical isomerization on MC crystal formation were also briefly described  
104 (Bayés-García et al., 2023). The analysis of the influence of the *cis-trans* isomerization on MC  
105 formation was performed by replacing *cis*-oleoyl to *trans*-elaidoyl (E) chains in the binary system of  
106 1,3-dipalmitoyl-2-elaidoyl glycerol (PEP)/1,3-dielaidoyl-2-palmitoyl glycerol (EPE) (Zhang et al.,  
107 2020).

108 The effects of MCs as polymorphic stabilizers of a third TAG component were discovered by  
109 Yoshikawa et al., who observed the crystallization kinetics in ternary mixtures of 1,3-distearoyl-2-  
110 oleoyl glycerol (SOS)/1,3-dioleoyl-2-stearoyl glycerol (OSO)/1,2,3-trilauroyl glycerol (LLL)  
111 (Yoshikawa et al., 2022). It was found that the most stable  $\beta$ -form of LLL was activated by the presence  
112 of  $\beta$ -crystals of  $MC_{SOS/OSO}$ . It was indicated that this work has a possibility to develop a new type of  
113 cocoa butter substitute (CBS).

114 Until recently, the application of MC formation to the end food products has been rather limited  
115 (Sibbald et al., 2016). However, systematic work was carried out to apply the MC-forming mixtures

116 to the development of cocoa butter equivalent (CBE) and cocoa butter substitute (CBS) formulations  
117 by forming the MC crystals in the ternary mixtures of cocoa butter, OSO, SSO and LLL fats (Watanabe  
118 et al., 2021; Watanabe et al., in submission). These studies may have indicated the high potential of  
119 the MC-forming TAG mixtures to produce the edible fats with novel functionality.

120

## 121 **Molecular-level understanding of the formation mechanisms of MC crystals**

122

123 Here briefly summarized are the main results of previous studies on the formation processes,  
124 structural properties and phase behavior of MC crystals.

125 It has been found that the following TAGs can form the MC crystals in their binary mixtures,  
126 in which the ratio of the component TAGs is always 50:50.

127  $S_{at}U_{S_{at}}$ : Symmetric saturated and unsaturated TAGs such as POP, SOS, PEP

128  $S_{at}S_{at}U$ : asymmetric saturated and unsaturated TAGs such as PPO (or OPP), SSO

129  $U_{S_{at}}U$ : symmetric unsaturated and saturated TAGs such as OPO, OSO, EPE

130  $U_{U_{S_{at}}}$ : asymmetric unsaturated and saturated TAGs such as OOS (or SOO) and OOP (or POO)

131 Figure 2 illustrates the combination of the TAGs, noting the MC-forming and eutectic mixtures.

132 In the binary mixtures of  $S_{at}U_{S_{at}}/S_{at}S_{at}U$  and  $S_{at}U_{S_{at}}/U_{S_{at}}U$ , the MC crystals are formed in the  
133 metastable  $\alpha$ ,  $\beta'$  and  $\beta$  polymorphs, as confirmed in the mixtures of SOS/OSO, SOS/SSO, POP/PPO,  
134 POP/PPO, PEP/EPE (see Introduction and section 3). However, the MC crystals are not formed and  
135 fully eutectic mixtures are formed in the combinations of  $S_{at}U_{S_{at}}/U_{U_{S_{at}}}$  and  $S_{at}S_{at}U/U_{S_{at}}U$ . The  
136 former result was confirmed in the mixtures of POP/OOP (Zhang et al., 2007) and SOS/OOS (Zhang  
137 et al., 2009), and the latter result was confirmed in the mixture of PPO/OPO (Bayés-García et al.,  
138 2015b).

139 Interestingly, the MC crystals were formed in the mixtures of  $U_{S_{at}}U/U_{U_{S_{at}}}$  and  $S_{at}S_{at}U/U_{U_{S_{at}}}$  in  
140 their metastable states. For example, the MC crystals in the OPO/OOP and PPO/OOP mixtures occurred

141 only under metastable conditions and tended to separate into component TAGs to form eutectic mixture systems  
142 after 17 months of storage (Bayés-García et al., 2015b). These results were in contrast to those of previous  
143 studies on  $S_{at}US_{at}/S_{at}S_{at}U$  and  $S_{at}US_{at}/US_{at}U$  in which the MC crystals are thermodynamically stable.

144 The molecular understanding of the ability and inability to form the MC crystals is still open to question.  
145 The main key factors may be the stabilization of chain packing between unsaturated and saturated chains,  $\pi$ - $\pi$   
146 interactions between the double bonds in the unsaturated chains and stabilization of glycerol conformations.

147 Figure 3 illustrates the glycerol conformations and structural models of the MC crystals by taking palmitic  
148 and oleic chains as  $S_{at}$  and U chains, respectively. The glycerol conformations are tuning fork in POP and OPO,  
149 and chair in PPO and OOP, and all the TAGs form triple chain length in their stable polymorphic forms of  $\beta$ -3  
150 in POP and OPO, and  $\beta'$ -3 in PPO and OOP (Bayés-García et al., 2015b, Floeter et al., 2018). Three  
151 problems may arise in the formation of the MC crystals of the double chain-length structure: the chain  
152 packing between palmitic and oleic chains, stacking of glycerol groups between the tuning fork and  
153 chair conformations, and the  $\pi$ - $\pi$  interactions between the unsaturated chains.

154 In the case of  $MC_{POP/OPO}$ , the stacking of the glycerol groups may be easily accomplished, since  
155 both component TAGs form the tuning fork conformation. The chain-chain packing including the  
156  $\pi$ - $\pi$  interactions may be easiest in  $MC_{POP/OPO}$ , and thus the formation of  $MC_{POP/OPO}$  can be easily done.

157 However, the stacking of the glycerol groups in  $MC_{POP/PPO}$  may be difficult since POP and PPO  
158 exhibit the tuning fork and chair conformations, respectively. In addition, steric hindrance between the  
159 oleic and palmitic chains may be a disturbing factor in the formation of  $MC_{POP/PPO}$ . Nevertheless, the  
160 metastable and stable polymorphs are formed in  $MC_{POP/PPO}$ . This suggests that the strong attractive  
161 interactions between palmitic chains may play dominant roles during the formation processes of  
162  $MC_{POP/PPO}$ .

163 In the case of  $MC_{OPO/OOP}$ , the stacking of the tuning fork (OPO) and chair (OOP) glycerol conformations  
164 may not be easy, and the chain packing between the palmitic and oleic chains is rather unstable. Therefore,  
165  $MC_{OPO/OOP}$  is not thermodynamically stable. In the case of PPO/OOP, it seems that both the chain packing and

166 the stacking of the chair glycerol conformation of PPO and OOP may enable the formation of MC crystals, but  
167  $MC_{PPO/OOP}$  is not thermodynamically stable. Finally, the structures of  $MC_{POP/OOP}$  and  $MC_{PPO/OPO}$  are unstable  
168 because the stacking of the glycerol groups and the chain packing may not stabilize the MC crystals. To conclude,  
169 the explanation of the formation of MC crystals at the molecular level seems to be incomplete except for  
170  $MC_{POP/OPO}$  and  $MC_{POP/PPO}$ , and further research is needed.

171 The crystallization kinetics of MC depends on the TAG molecular structures as well as the rate  
172 of cooling. For example, quite rapid cooling ( $> 40$  °C/min) of the binary mixture of POP/OPO resulted  
173 in separate crystallization of POP and OPO in the first, while  $MC_{POP/OPO}$  crystals started to form in  
174 addition to the POP and OPO crystals with decreasing cooling rates ( $<30$  °C/min). The extent of the  
175  $MC_{POP/OPO}$  crystals increased with decreasing cooling and heating rates after crystallization (Nakanishi  
176 et al., 2018). This result indicates that the formation of MC is a kinetic process involving competitive  
177 crystallization and structural rearrangement of the component TAGs.

178 Another interesting issue is the effect of racemization and optical isomerization of asymmetric  
179  $S_{at}S_{at}U$  and  $UUS_{at}$  on the formation of MC when mixed with other TAGs. For example, the phase  
180 behavior of  $POP/rac$ -PPO and  $OPO/sn$ -PPO is somewhat different in terms of the melting points of  
181  $MC_{POP/rac-PPO}$  and  $MC_{OPO/sn-PPO}$ , although both mixtures form stable polymorph of the double chain  
182 length structure ( $\beta$ -2). This may be related to the different crystallization kinetics of  $MC_{POP/rac-PPO}$  and  
183  $MC_{POP/sn-PPO}$  (see below).

184

### 185 **Formation of MC in binary mixtures of PEP/EPE**

186

187 Replacing the *cis* oleoyl chain in a TAG with a *trans* isomeric elaidoyl chain drastically changes  
188 its physical and even nutritional properties. However, very little is known about the actual crystal  
189 structures and phase behavior of elaidoyl-containing TAGs. To clarify the effect of *cis-trans*  
190 isomerization on the crystallization behavior of TAGs, the phase behavior of binary mixtures of 1,3-

191 dipalmitoyl-2-elaidoyl-glycerol (PEP) and 1,3-dielaidoyl-2-palmitoyl-glycerol (EPE) was investigated  
192 (Zhang et al., 2020). The binary mixtures of PEP and EPE were prepared at 10% intervals and  
193 characterized by DSC, conventional powder X-ray diffraction, and synchrotron radiation X-ray  
194 diffraction (SR-XRD). The effects of *cis-trans* isomerization on the crystallization behavior of  
195 TAGs were examined by comparison with related *cis* and fully saturated counterparts.

196 The most stable polymorphic forms are  $\beta'$  for PEP, but  $\beta$  for EPE (Zhang et al., 2020). The  
197 formation of MC crystals was first observed in the PEP/EPE mixture at a 50:50 ratio, as shown in the  
198 phase diagram (Figure 4). The PEP-rich region exhibited a monotectic phase for  $\beta$ -form MC and  
199  $\beta'$ -form PEP, whereas the EPE-rich region exhibited a monotectic phase for  $\beta$ -form MC and  $\beta$ -  
200 form EPE, which is quite similar to that observed for the POP/OPO (Minato et al. 1997).

201 The temperature dependence of the SR-XRD patterns and the DSC thermogram of PEP/EPE  
202 at a 50:50 ratio taken during cooling and heating at a rate of 2 °C/min is shown in Figure 5. The  
203 simultaneous crystallization of the  $\beta'$  form of  $MC_{PEP/EPE}$  along with the  $\alpha$  form was confirmed in  
204 the WAXS spectra by the appearance of  $\beta'$  peaks of 0.44 nm and 0.39 nm and an  $\alpha$  peak of 0.42 nm,  
205 as indicated by the arrows. With increasing temperature, the  $\alpha$  form transformed into the  $\beta'$  form  
206 and then further transformed to the thermodynamically stable  $\beta$  form via solid-state  
207 transformation. Then, the  $\beta$  form of MC melted at approximately 48 °C. In the SAXS spectra, the  
208 solid-state transition of  $\alpha \rightarrow \beta' \rightarrow \beta$  was confirmed by the shifting of the peak from 4.62 nm to 4.32  
209 nm and then to 4.25 nm.

210 Figure 6 shows the structural model of  $MC_{PEP/EPE}$  using the tuning fork conformation of  
211 glycerol group, which allows the void (see arrow) at the methyl end of PEP in  $\beta'$  form due to the  
212 chain length mismatch between neighboring P and E chains to be filled by the acyl chain of EPE, as

213 indicated by the dotted line. It is worth noting that when the “O” in certain binary mixtures of palmitic-  
214 oleic diacid TAGs such as POP and POO was replaced with “S”, or even “E”, the phase behavior  
215 remained the same. For example, a eutectic phase was found in both the POP/*rac*-POO (Zhang et al.,  
216 2007) and PSP/*rac*-PSS mixtures (Bhaggan et al., 2018), and the MC-forming mixture was formed in  
217 the POP/*rac*-PPO (Minato et al. 1997) and PSP/*rac*-PPS mixtures (Boodhoo et al., 2009). The MC-  
218 forming mixture was also found in the POP/OPO (Minato et al., 1997) and PEP/EPE mixtures (Zhang  
219 et al., 2020), and thus it is speculated that MC is formed in the PSP/SPS mixture.

220

### 221 **Crystallization kinetics of MC crystals of POP/OPO and POP/PPO**

222

223 To elucidate the effects of glycerol structures on the kinetic properties of MC-forming mixture  
224 phases, thermal analysis, X-ray diffraction and optical microscopy techniques were applied to the  
225 binary mixtures of POP/OPO, POP/*rac*-PPO and POP/1,2-dipalmitoyl-3-oleoyl-*sn*-glycerol (*sn*-PPO)  
226 (Bayés-García et al., 2023). All the three mixtures exhibited the MC-forming mixture at a 1:1 ratio.

227 The mixture samples were subjected to dynamic conditions of cooling at low and intermediate  
228 rates of 0.1, 0.5 and 2 °C/min to complete crystallization and reheating at a constant rate of 2 °C/min,  
229 while monitoring complex crystallization and polymorphic transition phenomena, as summarized in  
230 Figure 7. The POP/OPO mixture formed only MC<sub>POP/OPO</sub> crystals with double chain-length structure  
231 in its most stable  $\beta$  form when cooled under all the conditions analyzed, and they simply melted when  
232 heated. The occurrence of MC<sub>POP/OPO</sub>  $\beta$  form was reported in both pure liquid (Minato et al., 1997b)  
233 and *n*-dodecane solution systems (Ikeda et al., 2010).

234 Similarly, the most stable  $\beta$  form of MC<sub>POP/*rac*-PPO</sub> crystallized when cooled at 0.1 °C/min,  
235 although a metastable  $\beta'$  form was detected at 0.5 and 2 °C/min, which transformed to  $\beta$  when heated.

236 By contrast, the POP/*sn*-PPO mixture showed significantly complex polymorphic events in all  
237 the experimental conditions studied, showing the coexistence of  $MC_{POP/sn-PPO}$  with polymorphs of pure  
238 POP and *sn*-PPO component TAGs, even at the lowest cooling rate applied. In more detail, the 1:1  
239 TAGs mixture crystallized into  $\beta'$  forms of *sn*-PPO (triple chain length),  $MC_{POP/sn-PPO}$  (double chain  
240 length) and POP (double chain length) at 0.1 and 0.5 °C/min. When heated, the metastable  $\beta'$  of  
241  $MC_{POP/sn-PPO}$  transformed into its most stable  $\beta$  form before melting. At a higher cooling rate of  
242 2 °C/min, the least stable polymorphs predominated, showing complicated simultaneous  
243 crystallization processes of *sn*-PPO  $\beta'$  form (triple chain length) and  $\alpha$  forms (double chain length) of  
244  $MC_{POP/sn-PPO}$ , POP and *sn*-PPO. Subsequent heating caused polymorphic transformations of  $\alpha \rightarrow \beta' \rightarrow$   
245  $\beta$  for  $MC_{POP/sn-PPO}$ , and  $\alpha \rightarrow L \rightarrow \beta'$  for POP (see Figure 7).

246 Regarding the effects of optical isomerization in mixed systems of TAGs, extensive work had  
247 previously been carried out by Craven and Lenki (Craven et al., 2013). Additionally, Mizobe et al.  
248 analyzed the polymorphic structures of R-PPO, S-OPP and their mixtures, and concluded that the two  
249 optical isomers had identical structural properties, whereas the polymorphic characteristics of R-PPO  
250 and *rac*-PPO became different, with the latter corresponding to the 1:1 mixture of R-PPO/S-OPP  
251 (Mizobe et al., 2013).

252 To understand the differences in the crystallization behavior of  $MC_{POP/OPO}$  and  $MC_{POP/sn-OPO}$ , one  
253 can pay attention to their structural models, which are mainly based on the glycerol structures of POP,  
254 OPO and *sn*-PPO, as depicted in Figure 8. It can be assumed that the tuning fork glycerol conformation  
255 is the most stable one for both POP and OPO  $\beta$  forms, since the palmitic and oleic acid chains are  
256 located on different leaflets, favoring the packing of TAG molecules in triple chain-length structures  
257 that avoid the steric hindrance between straight palmitic and bent oleic acid chains. By contrast, the  
258 *sn*-PPO  $\beta'$  form may exhibit a chair-type glycerol conformation, which is also packed in a triple chain-  
259 length structure for the same reasons explained above.

260 During the formation process of the MC crystals, the chain-length structures were changed from  
261 triple to double, and close packing of glycerol groups and palmitic and oleic acid chains of neighboring  
262 TAG molecules occurred. A higher ability of  $MC_{POP/OPO}$  to form and stabilize in  $\beta$  form compared to  
263 other MCs was observed, since the tuning fork-type glycerol conformation of the two TAG  
264 components POP and OPO can be maintained in  $MC_{POP/OPO}$ , resulting in a  $\beta$ -2 structure with palmitic  
265 and oleic acid chains packed in separate leaflets. This ability was not observed in the POP/*sn*-PPO  
266 mixture, as it did not form  $MC_{POP/sn-PPO}$  alone, but it coexisted with single POP and *sn*-PPO TAG  
267 components.

268 Polarized light microscopy data confirmed a higher crystallization rate for *sn*-PPO crystals  
269 compared to other single TAGs or MCs, which may explain the separate crystallization when the  
270 POP/*sn*-PPO mixture was cooled, and this may also be explained from a structural point of view.  
271 According to our model (Figure 8), an extra molecular rearrangement may occur during the  $MC_{POP/sn-}$   
272 PPO formation, based on the change of the chair-type glycerol conformation of *sn*-PPO to the tuning  
273 fork-type, leading to an MC with coexisting oleic and palmitic acid chains in the same leaflet.

274 Regarding the different crystallization behavior of  $MC_{POP/sn-PPO}$  and  $MC_{POP/rac-PPO}$ , one may  
275 consider the ability of R-PPO and S-OPP to form a stable molecular packing (or racemic compound),  
276 which may interact with POP molecules to form a stable MC structure. However, further work may be  
277 required to understand the mechanisms involved.

278

### 279 **Interactive polymorphic crystallization of $MC_{SOS/OSO}$ and LLL**

280

281 The effect of MC formation on the polymorphic crystallization of the other coexisting TAG was  
282 examined using ternary TAG mixtures of LLL/SOS/OSO with a 1:1 weight ratio of SOS and OSO  
283 (SOS/OSO = 1/1) (Yoshikawa et al., 2022).

284 Under a series of thermal conditions of cooling from the melt, isothermal holding, and heating,  
285 pure LLL without containing SOS and OSO formed  $\beta'$  form crystals, which transformed to  $\beta$  form  
286 during the heating process after the crystallization. In 1992, it was found that the binary TAG mixture  
287 of SOS/OSO = 1/1 formed mainly  $\beta$ -form MC crystals of SOS and OSO ( $MC_{SOS/OSO}$ ) during the  
288 cooling process (Koyano et al., 1992). Based on these results, the ternary mixtures of LLL/SOS/OSO/  
289 at various mixing ratios of LLL and SOS/OSO=1/1 were investigated and the immiscible eutectic  
290 behavior was observed with retarded crystallization and lowered melting points of the formed crystals  
291 (Figure 9). Quite interesting results were found in the crystallization kinetics of two  $\beta$  forms of  
292  $MC_{SOS/OSO}$  and LLL; the  $\beta$  crystallization of  $MC_{SOS/OSO}$  coincided with the  $\beta'$  to  $\beta$  transformation or  
293 direct  $\beta$  melt-crystallization of LLL during the isothermal-holding process, as evident from the  
294 synchrotron radiation X-ray diffraction (SR-XRD) data shown in Figure 10. This coincidence strongly  
295 suggests the possibility that  $\beta$  crystallization of  $MC_{SOS/OSO}$  triggered the  $\beta$  crystallization of LLL. As a  
296 result, the spherulitic crystals of LLL deformed and changed their size distribution with increasing  
297 concentration of SOS/OSO=1/1. These peculiar phenomena of the interrelationships between the  
298 crystallization of  $\beta$  forms of  $MC_{SOS/OSO}$  and LLL have been defined as “interactive polymorphic  
299 crystallization” (Yoshikawa et al., 2022).

300 As a possible mechanism underlying the interactive polymorphic crystallization, epitaxial  
301 effects through triclinic-parallel ( $T_{//}$ ) subcell matching between  $\beta$  crystals of LLL and  $MC_{SOS/OSO}$  may  
302 occur in the same manner that  $\beta'$  form seed crystals of tripalmitin or tristearin effectively accelerated  
303  $\beta'$  crystallization of coconut oil through orthorhombic-perpendicular ( $O_{\perp}$ ) subcell matching  
304 (Mahisanunt et al., 2020). Another possible mechanism is martensitic transformation via cooperative  
305 displacement of atoms without diffusion in the crystal lattices, which can be initiated by the occurrence  
306 of local stress through mechanical or thermal stimulation, as indicated for petroselinic acid (Kaneko  
307 et al., 1997).

308 Elucidating the mechanism of interactive polymorphic crystallization requires further research,  
309 such as SR-XRD experiments substituting the component TAGs (LLL, SOS, and OSO) with the other  
310 corresponding TAGs (e.g., SSS, SSO, and SOO, respectively) and SR-XRD experiments using a  
311 microbeam technique to analyze the local orientation of TAG molecules near the crystal-crystal  
312 interfaces. For example, the SR-XRD data shown in Figure 11 indicate that the effect of facilitating  $\beta$   
313 crystallization of LLL in LLL/SOS/OSO was weakened by replacing OSO with rac-SOO, probably  
314 because SOS and SOO crystallized separately in the less stable forms of SOS 5L (2L + 3L), in which  
315 SOS formed in randomly packed double and triple chain-length structures (Mykhaylyk et al., 2007),  
316 and SOO  $\beta'$ .

317 It may be worth noting that the study of LLL/SOS/OSO mixtures can be applied to solve the  
318 problem of fat blooming in CBS-based compound coatings, which is partly caused by the polymorphic  
319 transformation of lauric acid-based TAG crystals in CBS from  $\beta'-2$  to  $\beta-2$  (see below).

320

### 321 **Application of MC crystals to new types of cocoa butter equivalent (CBE) and cocoa butter** 322 **substitute (CBS)**

323

324 Cocoa butter (CB) is indispensable ingredient in chocolate, as it is responsible for the physical  
325 properties such as hardness, texture, and melting behavior of chocolate products (Talbot, 2017).  
326 However, CB is one of the most expensive ingredients of chocolate and its price is gradually  
327 increasing due to several global issues such as low productivity of cacao due to climate change and  
328 increasing demand for cacao products (Afoakwa, 2016). Therefore, the confectionery industry has  
329 developed CB alternative fats (CBAs) with various functionalities to replace or blended with CB in  
330 chocolate production.

331 CBAs can be classified into three groups based on their compositions: cocoa butter equivalent  
332 (CBE), cocoa butter replacer (CBR) and cocoa butter substitute (CBS) (Timms, 2003). Recently, two  
333 experimental studies on the physical properties and fat bloom stability of chocolate made with  
334  $S_{at}S_{at}U$  and  $US_{at}U$  type fats forming MC crystals with CB revealed that these fats can be used as new  
335 types of CBA fats (Watanabe et al., 2021., Watanabe et al., in submission).

336

### 337 **CBE**

338 Systematic studies showed that the ternary mixtures of SOS, *rac*-SSO and OSO form MC  
339 crystals of stable  $\beta$ -2 form at a concentration of SOS of 50% with different concentrations of SSO  
340 and OSO (Watanabe et al., 2018). Figure 12 shows that the MC crystals with the stable  $\beta$ -2  
341 polymorph are formed in a series of the ternary mixtures of SOS/SSO/OSO, in which the ratio of  
342  $SOS/(SSO+OSO)$  was set to 50/50 and the ratio of SSO/OSO was varied. Based on this study, it was  
343 expected that the ternary mixtures can produce a new type of CBE with the stable polymorphic  
344 structure when SOS, SSO and OSO are replaced with CB, SSO-fat and OSO-fat. The SSO-fat and  
345 OSO-fat were prepared by full-hydrogenation, interesterification, and fractionation of canola oil high  
346 oleic sunflower oil (Watanabe et al., 2021). The physical properties and fat bloom stability of  
347 chocolates containing SSO-fat and OSO-fats, which were solidified by simple cooling without  
348 tempering process, were then evaluated (Watanabe et al., 2021).

349 It should be noted that in the chocolate fat phases, the final ratio of the three types of TAG,  
350  $S_{at}US_{at}/S_{at}S_{at}U/US_{at}U$ , were 50/50/0–50/0/50. Figure 13 shows the temperature change in solid fat  
351 content (SFC) values of six fat blends and CB, where the concentrations (%) of  $S_{at}US_{at}/S_{at}S_{at}U/US_{at}U$   
352 in the fat blends are 50/46/4 (sample A), 50/40/10 (B), 50/30/20 (C), 50/20/30 (D), 50/10/40 (E), and  
353 50/3/47 (F). The SFC measurement of ternary fat blends of CB, SSO-fat and OSO-fat showed sharp

354 melting profiles around body temperature. Similarly, in the hardness measurement chocolate samples  
355 prepared with fat blends of  $S_{at}U S_{at}/S_{at}S_{at}U/US_{at}U=50/30/20-50/20/30$  showed almost the same  
356 hardness as that of pure chocolate. In addition, no fat bloom formation was observed in dark chocolate  
357 with the fat blends of  $S_{at}U S_{at}/S_{at}S_{at}U/US_{at}U$  of  $50/20/30-50/0/50$  during the one-year storage under  
358 isothermal condition at 25 °C and thermal cycling condition between 20 and 30 °C. Overall, the CB,  
359 SSO-fat, and OSO-fat blends can be used as a cocoa butter equivalent (CBE) without tempering  
360 procedures.

361

## 362 **CBS**

363 The MC crystals made of CB and OSO-fat ( $MC_{CB/OSO}$ ) were applied to compound chocolate  
364 formulations by blending with lauric cocoa butter substitutes (CBS) (Watanabe et al., in submission).  
365 Conventional CBSs have been produced by fractionation, hydrogenation and a combination of these  
366 processes of lauric fats derived from palm kernel oil and other natural fats (Rossell, 1985). These fats  
367 are composed of TAGs with lauric (L) and myristic (M) acid moieties including LLL, LLM, LMM,  
368 and MMM which are crystallized into  $\beta'-2$  form by simple cooling without tempering (Smith, 2012).  
369 However, the CBS-based chocolate can potentially convert from the  $\beta'-2$  to  $\beta-2$  form, which leads to  
370 fat bloom formation during long-term storage, because mono-acid TAGs such as LLL and MMM  
371 have the potential to transform from  $\beta'-2$  to the more stable  $\beta-2$  form ( $\beta$ -tending; Koizumi et al.,  
372 2022). In addition, cacao solids such as cacao powder and cacao liquor are often blended to improve  
373 the flavour and taste of compound chocolate, resulting in more serious fat bloom due to the phase  
374 separation of CBS and CB followed by polymorphic transformation of CB TAGs. This eutectic  
375 effect makes it difficult to blend more than 5% cocoa butter in the compound chocolates (Laustsen,  
376 1991).

377 As described in the previous section, studies on the polymorphic crystallization behavior of the  
 378 ternary mixture system of LLL/SOS/OSO with the SOS/OSO ratio of 1/1 have revealed that the  
 379 crystallization of  $\beta$ -2 form in  $MC_{SOS/OSO}$  promoted the crystallization and polymorphic transformation  
 380 of  $\beta'$ -2 to  $\beta$ -2 in LLL (Yoshikawa et al., 2022). Based on these results, the physical properties and fat  
 381 bloom stability of lauric-based compound chocolate with  $MC_{CB/OSO}$  were evaluated.

382 Table 1 shows six chocolate samples with the different relative concentrations (%) of CBS, OSO-  
 383 fat and CB investigated. The SFC studies showed that the fat blends of CBS and  $MC_{CB/OSO}$  exhibited  
 384 immiscible eutectic behavior, as did the fat blends of CBS and CB. The results of SFC value,  
 385 crystallization rates and hardness of compound chocolate with  $MC_{CB/OSO}$  suggested that the compound  
 386 chocolate is suitable for the chocolate production up to about 20% of  $MC_{CB/OSO}$  in the fat phases.

387

388 Table 1. Relative concentrations (%) of CBS, CB and OSO-fat in total chocolate fat in eight  
 389 chocolate samples

Sample	CBS	OSO-fat	CB
A1	90.0	0.0	10.0
A2	85.0	0.0	15.0
A3	80.0	0.0	20.0
A4	75.0	0.0	25.0
B1	80.0	10.0	10.0
B2	70.0	15.0	15.0
B3	60.0	20.0	20.0
B4	50.0	25.0	25.0

390

391 In the fat bloom evaluation studies, while CBS/CB compound chocolate exhibited severe fat  
 392 bloom within a few weeks, the CBS/CB/OSO-fat compound chocolate showed no fat bloom under any  
 393 storage condition for 6 months (Table 2). In addition, the XRD studies revealed that no polymorphic  
 394 transformation occurred for the CBS/CB/OSO-fat blends during the 6 months storage, while the  
 395 polymorphic transformation from  $\beta'$ -2 to  $\beta$ -2 was observed for the fat blends of CBS/CB. The  
 396 polymorphic transformations of CB TAGs and  $\beta$ -tending TAG in CBS cause fat blooming in CBS-  
 397 based compound chocolate. Therefore, the mechanisms of fat blooming inhibition in compound  
 398 chocolate made of CBS/CB/OSO-fat summarized in Table 1 can be assumed that  $\beta$ -tending TAG  
 399 fractions in the CBS, such as LLL and MMM, may crystallize into  $\beta$ -form during the cooling process  
 400 via interactive polymorphic crystallization with  $MC_{CB/OSO}$ . However, further studies are required to  
 401 elucidate these mechanisms.

402

403 Table 2. Evaluation of fat bloom formation of eight dark chocolate samples after storage for 3 weeks  
 404 (3W) and 15 weeks (15W) under different thermal conditions, -; no fat bloom, +; slightly bloomed,  
 405 ++; fairly bloomed, +++: seriously bloomed

Chocolate sample	15°C		20°C		25°C		15-25°C	
	3W	15W	3W	15W	3W	15W	3W	15W
A1	+	+++	+	++	-	++	-	+
A2	+	+++	+	++	-	++	-	+
A3	+	+++	+	++	+	++	-	+
A4	+	+++	+	++	+	++	-	+
B1	-	-	-	-	-	-	-	-
B2	-	-	-	-	-	-	-	-
B3	-	-	-	-	-	-	-	-
B4	-	-	-	-	-	-	-	-

406

## 407 **CONCLUSION**

408

409 The study of the mixing behavior of principal TAGs and various natural and industrialized fats  
410 is of great importance, as it is one of the most informative and applicable studies to improve the  
411 physicochemical properties of lipid-based products using natural and technologically-produced lipid  
412 materials. Until recently, the phases of MC-forming mixture have been studied from a fundamental  
413 point of view using pure samples of saturated-unsaturated mixed-acid TAGs. However, the fat  
414 materials produced by full-hydrogenation, interesterification and fractionation of vegetable fats and  
415 oils have been used for the application of the MC crystals to end products such as fat spreads and  
416 confectionery fats. The physical properties of the MC crystals are different from those of the  
417 component TAGs and can improve the end products when applied; for example, the formation of MC  
418 crystals containing the mixed acid TAGs with oleic acid moiety can reduce the use of saturated fats  
419 (Sibbald et al., 2016), and the application of the MC crystals containing CB, OSO-fat, and SSO-fat to  
420 CBE and CBS improved the crystallization kinetics and fat bloom stability. It is expected to explore  
421 the molecular mechanisms of the ability and inability of MC formation, and the application of the MC  
422 crystals to other end products such as emulsified and aerated systems.

423

## 424 **AUTHOR CONTRIBUTIONS**

425

426 LB, KT, LZ, SY, FK, YY and SW performed the experiments and published their original articles,  
427 which are reviewed in this article. KS initiated and organized this work.

428

## 429 **ACKNOWLEDGMENTS**

430

431 The acknowledgment is given to the National Natural Science Foundation of China (Grant No.  
432 31401661) and the Photon Factory Program Advisory Committee (Proposal No. 2017G648 &  
433 2018G092), whose support enabled to perform the experiments shown in Figures 4 and 5. The  
434 acknowledgment is also given to the Photon Factory Program Advisory Committee (Proposal No.  
435 2019G065 and 2021G049), whose support enabled us to perform the experiments shown in Figures10  
436 and 11. The study on MC crystals of POP/OPO and POP/PPO (Figures 7 and 8) was supported by the  
437 Generalitat de Catalunya through project 2021 SGR 00262, and Grant PID2019-107032RB-I00 funded  
438 by MCIN/AEI/10.13039/501100011033/.

439 **Figure caption**

440

441 **Figure 1** Typical three binary mixing systems of triacylglycerols (TAGs). A and B: component  
442 TAGs, L; liquid phase,  $S_A$ ,  $S_B$  and  $S_{MC}$ ; solid phases of A, B and molecular compound (MC).

443

444 **Figure 2** Combination of saturated ( $S_{at}$ )-unsaturated (U) mixed-acid TAGs exhibiting MC-  
445 forming and eutectic binary mixtures.

446

447 **Figure 3** Key factors affecting the formation of MC crystals in binary mixtures of TAGs  
448 containing palmitic (P) and oleic (O) acid moiety.

449

450 **Figure 4** Mixing phase behavior of PEP and EPE.

451

452 **Figure 5** DSC thermogram and SR-XRD patterns of PEP/EPE at a 50:50 ratio.

453

454 **Figure 6** Possible mechanism of  $MC_{PEP/EPE}$  formation.

455

456 **Figure 7** Summary of temperature-dependent polymorphic crystallization in the binary mixtures  
457 of POP/OPO, POP/*rac*-PPO and POP/*sn*-PPO.

458

459 **Figure 8** Effects of chain packing and glycerol conformation on the formation of MC crystals.

460

461 **Figure 9** Phase behavior of LLL/SOS/OSO mixtures with different weight fractions of  
462 SOS/OSO = 1/1 ( $W_{\text{SOS/OSO}}$ ): melting of  $\text{MC}_{\text{SOS/OSO}} \beta\text{-2}$  ( $\square$ ), transformation  $\beta\text{-2} \rightarrow \beta\text{-2}$  of LLL ( $\blacktriangle$ ),  
463 and melting of LLL  $\beta\text{-2}$  ( $\bullet$ ).

464

465 **Figure 10** 3D surface plots and overhead projections of SR-XRD data on LLL/SOS/OSO =  
466 2/1/1 (a) and 1/2/2 (b), taken during cooling at a rate of 2 °C/min, holding at 15 °C for 30 min, and  
467 heating at a rate of 5 °C/min. Numbers hyphenated to Greek letters for crystal polymorphs represent  
468 the chain-length structure. Unit: nm.

469

470 **Figure 11** 3D surface plots and overhead projections of SR-XRD data on LLL/SOS/*rac*-SOO =  
471 2/1/1, taken during cooling at a rate of 2 °C/min, holding at 15 °C for 30 min, and heating at a rate of  
472 5 °C/min. Numbers hyphenated to Greek letters for crystal polymorphs represent the chain-length  
473 structure. Unit: nm.

474

475 **Figure 12** Phase diagram of ternary mixture systems of SOS/SSO/OSO. White symbols  
476 represent MC crystals of  $\beta\text{-2}$ , black symbols represent eutectic mixtures of  $\beta\text{-2}$  of MC crystals and  
477 component TAG.

478

479 **Figure 13** SFC profiles of CB and CB/SSO-fat/OSO-fat blends. Blending ratio of A–F are as  
480 follows. CB/SSO-fat/OSO-fat = (A) 50/50/0, (B) 50/40/10, (C) 50/30/20, (D) 50/20/30, (E) 50/10/40  
481 and (F) 50/0/50.

482

## 483 REFERENCES

484

485 Acevedo NC, Block JM, Marangoni AG. Unsaturated emulsifier mediated modification of the  
486 mechanical strength and oil binding capacity of a model edible fat crystallized under shear.  
487 *Langmuir*. 2012; 28:16207–16217. <https://doi.org/10.1021/la303365d>

488

489 Acevedo NC, Marangoni AG. Functionalization of noninteresterified mixtures of fully hydrogenated  
490 fats using shear processing. *Food Bioprocess Technology*. 2014;7:575–587.  
491 <https://doi.org/10.1007/s11947-013-1110-z>

492

493 Afoakwa EO. World cocoa production, processing and chocolate consumption pattern. In: Afoakwa  
494 EO. editor. *Chocolate Science and Technology*. West Sussex, UK: Wiley & Blackwell; 2016. p.  
495 17–48

496

497 Alishevich K, Berčíková M, Kyselka J, Sasínová K, Honzíkova T, Šimicová P, Šmidrkal J, Rohlíček  
498 J, Filip V. Binary Phase Behavior of 2-oleoyl-1-palmitoyl-3-stearoyl-rac-glycerol (POS) and  
499 2-linoleoyl-1-palmitoyl-3-stearoyl-rac-glycerol (PLS). *Food Biophysics*. 2023;18:161–173.  
500 <https://doi-org.sire.ub.edu/10.1007/s11483-022-09761-8>

501

502 Bhaggan K, Smith KW, Blecker C, Danthine S. Polymorphism and Kinetic Behavior of Binary  
503 Mixtures of Trisaturated Triacylglycerols Containing Palmitic and Stearic Acid Under Non-  
504 Isothermal Conditions. *European Journal of Lipid Science and Technology*. 2018;120:1800072.  
505 <https://doi.org/10.1002/ejlt.201800072>  
506

507 Bayés-García L, Calvet T, Cuevas-Diarte MA, Ueno S, Sato K. Crystallization and Transformation of  
508 Polymorphic Forms of Trioleoyl Glycerol and 1,2-Dioleoyl-3-*rac*-linoleoyl Glycerol. *Journal of*  
509 *Physical Chemistry B*. 2013;117:9170–9181. <https://doi.org/10.1021/jp403872a>  
510

511 Bayés-García L, Patel AR, Dewettinck K, Rousseau D, Sato K, Ueno S. Lipid crystallization kinetics  
512 - roles of external factors influencing functionality of end products. *Current Opinion in Food*  
513 *Science*. 2015a;4: 32–38. <https://doi.org/10.1016/j.cofs.2015.04.005>  
514

515 Bayés-García L, Calvet T, Cuevas-Diarte MA, Ueno S, Sato K. Phase Behavior of Binary Mixture  
516 Systems of Saturated-Unsaturated Mixed-Acid Triacylglycerols: Effects of Glycerol Structures  
517 and Chain-Chain Interactions. *Journal of Physical Chemistry B*. 2015b;119:4417–4427.  
518 <https://doi.org/10.1021/acs.jpcc.5b00673>  
519

520 Bayés-García L, Calvet T, Cuevas-Diarte MA, Ueno S. In situ crystallization and transformation  
521 kinetics of polymorphic forms of saturated-unsaturated-unsaturated triacylglycerols: 1-palmitoyl-  
522 2,3-dioleoyl glycerol, 1-stearoyl-2,3-dioleoyl glycerol, and 1-palmitoyl-2-oleoyl-3-linoleoyl  
523 glycerol. *Food Research International*. 2016;85:244–258.  
524 <https://doi.org/10.1016/j.foodres.2016.05.011>  
525

526 Bayés-García L, Calvet T, Cuevas-Diarte MA, Ueno S. From Trioleoyl glycerol to extra virgin olive  
527 oil through multicomponent triacylglycerol mixtures: Crystallization and polymorphic  
528 transformation examined with differential scanning calorimetry and X-ray diffraction techniques.  
529 Food Research International. 2017;99: 476–484. <https://doi.org/10.1016/j.foodres.2017.06.015>  
530

531 Bayés-García L, Calvet T, & Cuevas-Diarte MA. Effects of dynamic temperature variations on  
532 microstructure and polymorphic behavior of lipid systems. In Sato K editor. Crystallization of  
533 lipids. Fundamentals and applications in food, cosmetics and pharmaceuticals. Hoboken, NJ,  
534 USA: Wiley-Blackwell; 2018. p. 183–210. <https://doi.org/10.1002/9781118593882.ch6>  
535

536 Bayés-García L, Yoshikawa S, Aguilar-Jiménez M, Ishibashi C, Ueno S, Calvet T. Heterogeneous  
537 Nucleation Effects of Talc Particles on Polymorphic Crystallization of Cocoa Butter. Crystal  
538 Growth & Design. 2022;22:213–227. <https://doi.org/10.1021/acs.cgd.1c00859>  
539

540 Bayés-García L, Fukao K, Konishi T, Sato K, & Taguchi K. Crystallization and Transformation  
541 Behavior of Triacylglycerol Binary Mixtures Forming Molecular Compounds of POP/OPO,  
542 POP/rac-PPO, and POP/sn-PPO. Crystal Growth & Design. 2023;23:2870–2881.  
543 <https://doi.org/10.1021/acs.cgd.3c00038>  
544

545 Boodhoo MV, Bouzidi L, Narine SS. The binary phase behavior of 1, 3-dipalmitoyl-2-stearoyl-sn-  
546 glycerol and 1, 2-dipalmitoyl-3-stearoyl-sn-glycerol. Chemistry and Physics of Lipids.  
547 2009;160:11–32. <https://doi.org/10.1016/j.chemphyslip>  
548

549 Chen F, Zhang H, Sun X, Wang X, & Xu X. Effects of ultrasonic parameters on the crystallization  
550 behavior of palm oil. *Journal of the American Oil Chemists' Society*. 2013;90:941–949.  
551 <https://doi.org/10.1007/s11746-013-2243-y>  
552

553 Cholakova, D, Tcholakova, S, & Denkov, N. Polymorphic Phase Transitions in Bulk Triglyceride  
554 Mixture. *Crystal Growth & Design*. 2023;23:2075–2091. <https://doi.org/10.1021/acs.cgd.2c01021>.  
555

556 Craven RJ, Lencki RW. Polymorphism of Acylglycerols: A Stereochemical Perspective. *Chemical*  
557 *Review*. 2013;113:7402–7420. <https://doi.org/10.1021/cr400212r>  
558

559 Douaire M, di Bari V, Norton JE, Sullo A, Lillford P, Norton IT. Fat crystallisation at oil-water  
560 interfaces. *Advances in Colloid and Interface Science*. 2014;203:1–10.  
561 <https://doi.org/10.1021/acs.cgd.2c01021>  
562

563 Floeter E, Haeupler M, Sato K. Molecular interactions and mixing phase behavior of lipid crystals. In  
564 Sato K editor. *Crystallization of lipids. Fundamentals and applications in food, cosmetics and*  
565 *pharmaceuticals*; Hoboken, NJ, USA: Wiley-Blackwell; 2018. p. 61–104.  
566 <https://doi.org/10.1002/9781118593882.ch3>  
567

568 Gibon V, Durant F, Deroanne C. Polymorphism and intersolubility of some palmitic, stearic and oleic  
569 triglycerides: PPP, PSP and POP. *Journal of the American Oil Chemists' Society*. 1986;63:1047–  
570 1055. <https://doi.org/10.1007/BF02673796>  
571

572 Gibon V, Danthine S. Systematic Investigation of Co-Crystallization Properties in Binary and Ternary  
573 Mixtures of Triacylglycerols Containing Palmitic and Oleic Acids in Relation with Palm Oil Dry  
574 Fractionation. *Foods*. 2020;9:1891. <https://doi.org/10.3390/foods9121891>  
575

576 Ghazani SM, Marangoni AG. The ternary solid state phase behavior of triclinic POP, POS and SOS  
577 and its relationship to CB and CBE properties. *Crystal Growth & Design*. 2019a;19:704–713.  
578 <https://doi.org/10.1021/acs.cgd.8b01273>  
579

580 Ghazani, S.M., & Marangoni, A. G. The triclinic polymorphism of cocoa butter is dictated by its major  
581 molecular species, 1-palmitoyl, 2-oleoyl, 3-stearoyl glycerol (POS). *Crystal Growth & Design*.  
582 2019b;19: 90–97. <https://doi.org/10.1021/acs.cgd.8b00973>  
583

584 Gresti J, Bugaut M, Maniongui C, Bezard, J. Composition of molecular species of triacylglycerols in  
585 bovine milk fat. *Journal of Dairy Science*. 1993;76:1850–1869. [https://doi.org/10.3168/jds.S0022-  
586 0302\(93\)77518-9](https://doi.org/10.3168/jds.S0022-0302(93)77518-9)  
587

588 Ikeda E, Ueno S, Miyamoto R, Sato K. Phase Behavior of a Binary Mixture of 1,3-dipalmitoyl-2-  
589 oleoyl-sn-glycerol and 1,3-dioleoyl-2-palmitoyl-sn-glycerol in n-dodecane Solution. *Journal of*  
590 *Physical Chemistry B*. 2010;114:10961–10969. <https://doi.org/10.1021/jp101821c>  
591

592 Ikeda-Naito E, Hondoh H, Ueno S, Sato K. Mixing phase behavior of 1,3-dipalmitoyl-2-oleoyl-  
593 sn-glycerol (POP) and 1,2-dipalmitoyl-3-oleoyl-rac-glycerol (PPO) in n-dodecane solution.  
594 *Journal of the American Oil Chemists' Society*. 2014;91:1837–1848.  
595 <https://doi.org/10.1007/s11746-014-2534-y>  
596

597 Joshi BL, Zielbauer BI, Vilgis TA. Comparative Study on Mixing Behavior of Binary Mixtures of  
598 Cocoa Butter/Tristearin (CB/TS) and Cocoa Butter/Coconut Oil (CB/CO). *Foods*. 2020;9: 327.  
599 <https://doi.org/10.3390/foods9030327>  
600

601 Kaneko F, Kobayashi M, Sato K, Suzuki M. Martensitic phase transition of petroselinic acid:  
602 influence of polytypic structure. *Journal of Physical Chemistry B*. 1997;101:285–292.  
603 <https://doi.org/10.1021/jp9625927>  
604

605 Koizumi H, Takagi M, Hondoh H, Michikawa S, Hirai Y, Ueno S. Control of Phase Separation for  
606 CBS-Based Compound Chocolates Focusing on Growth Kinetics. *Crystal Growth & Design*.  
607 2022;22:6879–6885. <https://doi.org/10.1021/acs.cgd.2c00317>  
608

609 Koyano T, Hachiya I, Sato K. Phase Behavior of Mixed Systems of SOS and OSO. *Journal of Physical*  
610 *Chemistry*. 1992;96:10514–10520. <https://doi.org/10.1021/j100204a072>  
611

612 Koyano T, Kato Y, Hachiya I, Unemura R. Crystallization behavior of ternary mixture of  
613 POP/POS/SOS. *Journal of the Japanese Oil Chemists' Society*. 1993;42:453–457.  
614 <https://doi.org/10.5650/jos1956.42.453>  
615

616 Larsson K, Quinn P, Sato K, Tiberg F. *Lipids: Structure, Physical Properties and Functionality*. Oily  
617 Press: Bridgwater, U.K.; 2006  
618

619 Laustsen K. The nature of fat bloom in molded compound coatings. *The Manufacturing*  
620 *Confectioner*. 1991;71,137–144

621

622 Lee J, Ye Y, Martini S. Physicochemical and oxidative changes in sonicated interesterified soybean  
623 oil. *Journal of the American Oil Chemists' Society*. 2015;92:305–308.  
624 <https://doi.org/10.1007/s11746-014-2585-0>

625

626 Lu C, Zhang B, Zhang H, Guo Y, Dang L, Liu Z, Shu Q, Wang Z. Solid–liquid phase equilibrium and  
627 phase behaviors for binary mixtures composed of tripalmitoylglycerol (PPP), 1,3-dipalmitoyl-2-  
628 oleoylglycerol (POP), and 1,2-dioleoyl-3-palmitoyl-glycerol (POO). *Industrial and Engineering*  
629 *Chemical Research*. 2019;58:10044–10052. <https://doi.org/10.1021/acs.iecr.9b01947>

630

631 Lusi M. A rough guide to molecular solid solution: Design, synthesis and characterization of mixed  
632 crystals. *Crystal Engineering Communication*. 2018;20:7042–7052.  
633 <https://doi.org/10.1039/C8CE00691A>

634

635 Macridachis J, Bayés-García L, Calvet T. An Insight into the Solid-State Miscibility of Triacylglycerol  
636 Crystals. *Molecules*, 2020;25:4562. <https://doi.org/10.3390/molecules25194562>

637

638 Macridachis J, Bayés-García L, Calvet T. Mixing Phase Behavior of Tripalmitin and Oleic-Rich  
639 Molecular Compound-Forming Triacylglycerols. *Industrial and Engineering Chemical Research*.  
640 2021;60:5374–5384. <https://doi.org/10.1021/acs.iecr.1c00324>

641

642 Macridachis J, Bayés-García L, Calvet T. Solid phase behavior of mixture systems based on  
643 tripalmitoyl glycerol and monounsaturated triacylglycerols forming a molecular compound.  
644 *Physical Chemistry and Chemical Physics*. 2022;24:3749–3760.  
645 <https://doi.org/10.1039/D1CP05361B>

646

647 Mahisanunt B, Hondoh H, Ueno S. Coconut oil crystallization on tripalmitin and tristearin seed

648 crystals with different polymorphs. *Crystal Growth & Design*. 2021;20:4980–4990.

649 <https://doi.org/10.1021/acs.cgd.0c00064>

650

651 Mao J, Gao Y, Meng Z. Crystallization and phase behavior in mixture systems of anhydrous milk

652 fat, palm stearin, and palm oil: Formation of eutectic crystals. *Food Chemistry*. 2023;399:133877.

653 <https://doi.org/10.1016/j.foodchem.2022.133877>

654

655 Martini S. Sonocrystallization of fats. In: *Sonocrystallization of Fats*. SpringerBriefs in Food, Health,

656 and Nutrition. Springer, New York, NY; 2013. [https://doi.org/10.1007/978-1-4614-7693-1\\_6](https://doi.org/10.1007/978-1-4614-7693-1_6)

657

658 Mazzanti G, Li M, Marangoni AG, Idziak SHJ. Effects of shear rate variation on the nanostructure of

659 crystallizing triglycerides. *Crystal Growth & Design*. 2011;11:4544–4550.

660 <https://doi.org/10.1021/cg200786k>

661

662 Minato A, Ueno S, Yano J, Wang ZH, Seto H, Amemiya Y, Sato K. Synchrotron radiation X-ray

663 diffractions study on phase behavior of PPP-POP binary mixtures. *Journal of the American Oil*

664 *Chemists' Society*. 1996;73:1567–1572. <https://doi.org/10.1007/BF02523526>

665

666 Minato A, Ueno S, Smith K, Amemiya Y, Sato K. Thermodynamic and Kinetic Study on Phase

667 Behavior of Binary Mixtures of POP and PPO Forming Molecular Compound Systems. *Journal*

668 *of Physical Chemistry B*. 1997a;101: 3498–3505. <https://doi.org/10.1021/jp962956v>

669

670 Minato A, Ueno S, Yano J, Smith K, Seto H, Amemiya Y, Sato K. Thermal and Structural Properties  
671 of sn-1,3-dioleoyl-2-palmitoylglycerol Binary Mixtures Examined with Synchrotron Radiation X-  
672 Ray Diffraction. *Journal of the American Oil Chemists' Society*. 1997b;74:1213–1220.  
673 <https://doi.org/10.1007/s11746-997-0047-7>  
674

675 Minato A, Yano J, Ueno S, Smith K, Sato K. FT-IR study on microscopic structures and conformations  
676 of POP-PPO and POP-OPO molecular compounds. *Chemistry and Physics of Lipids*.  
677 1997c;88:63–71. [https://doi.org/10.1016/S0009-3084\(97\)00045-5](https://doi.org/10.1016/S0009-3084(97)00045-5)  
678

679 Mizobe H, Tanaka T, Hatakeyama N, Nagai T, Ichioka K, Hondoh H, Ueno S, Sato K. Structures and  
680 binary mixing characteristics of enantiomers of 1-oleoyl-2,3-dipalmitoyl-sn-glycerol (S-OPP) and  
681 1,2-dipalmitoyl-3-oleoyl-sn-glycerol (R-PPO). *Journal of the American Oil Chemists' Society*.  
682 2013;90:1809–1817. <https://doi.org/10.1007/s11746-013-2339-4>  
683

684 Myher JJ, Kuksis A, Marai L, Sandra P. Identification of the more complex triacylglycerols in bovine  
685 milk fat by gas chromatography-mass spectrometry using polar capillary columns. *Journal of*  
686 *Chromatography*. 1988;452: 93–118. [https://doi.org/10.1016/S0021-9673\(01\)81440-0](https://doi.org/10.1016/S0021-9673(01)81440-0)  
687

688 Mykhaylyk OO, Smith KW, Martin CM, Ryan AJ. Structural models of metastable phases occurring  
689 during the crystallization process of saturated/unsaturated triacylglycerols. *Journal of Applied*.  
690 *Crystallography*. 2007;40: 297–302. <https://doi.org/10.1107/S0021889806055191>  
691

692 Nakanishi K, Mikiya Y, Ishiguro T, Ueno S. Crystallization behavior of molecular compound in binary  
693 mixture system of 1,3-dioleoyl-2-palmitoyl-sn-glycerol and 1,3-dipalmitoyl-2-oleoyl-sn-glycerol.

694 Journal of the American Oil Chemists' Society. 2018;95:51–59.  
695 <https://doi.org/10.1002/aocs.12005>  
696  
697 Povey MJW. Crystal nucleation in food colloids. *Food Hydrocolloids*. 2014;42:118–129.  
698 <https://doi.org/10.1016/j.foodhyd.2014.01.016>  
699  
700 Rossell JB. Fractionation of lauric oils. *Journal of the American Oil Chemists' Society*. 1985;62:385–  
701 390. <https://doi.org/10.1007/BF02541409>  
702  
703 Rousset P, Rappaz M, Minner E. Polymorphism and solidification kinetics of the binary system  
704 POS/SOS. *Journal of the American Oil Chemists' Society*. 1998;75:857–864.  
705 <https://doi.org/doi:10.1007/s11746-998-0237-y>  
706  
707 Sasaki M, Ueno S, Sato K. Polymorphism and mixing phase behavior of major triacylglycerols of  
708 cocoa butter. In: Garti N, Widlak NR, editors. *Cocoa butter and related compounds*. AOCS Press:  
709 Urbana, IL, USA; 2012. p. 151–172. <https://doi.org/10.1016/B978-0-9830791-2-5.50009-8>  
710  
711 Seilert J, Moorthy AS, Kearsley AJ, Floeter E. Revisiting a model to predict pure triglyceride  
712 properties: parameter optimization and performance. *Journal of the American Oil Chemists'*  
713 *Society*. 2021;98:837–850. <https://doi.org/10.1002/aocs.12515>  
714  
715 Sibbald AN, Carney JR, Marangoni AG. Enhanced Structuring of Fat with Reduced Saturates Using  
716 Mixed Molecular Compounds. *Journal of the American Oil Chemists' Society*. 2016;93:1441–  
717 1452. <https://doi.org/10.1007/s11746-015-2718-0>

718

719 Smith KW. Confectionery Fats. In: Garti N, Widlak NR, editors. Cocoa butter and related  
720 compounds. AOCS Press: Urbana, IL, USA; 2012. p. 475–495. [https://doi.org/10.1016/B978-0-](https://doi.org/10.1016/B978-0-9830791-2-5.50022-0)  
721 [9830791-2-5.50022-0](https://doi.org/10.1016/B978-0-9830791-2-5.50022-0)

722

723 Smith KW, Bhaggan K, Talbot G, van Malsen K. Crystallization of lipids: influence of minor  
724 components and additives. *Journal of the American Oil Chemists' Society*. 2011;88:1085–1101.  
725 <https://doi.org/10.1007/s11746-011-1819-7>

726

727 Sonwai S, Mackley MR. The effect of shear on the crystallization of cocoa butter. *Journal of the*  
728 *American Oil Chemists' Society*. 2006;83:583–596. <https://doi.org/10.1007/s11746-006-1243-6>

729

730 Takeuchi M, Ueno S, Sato K. Crystallization kinetics of polymorphic forms of a molecular compound  
731 constructed by SOS (1,3-distearoyl-2-oleoyl-sn-glycerol) and SSO (1,2-distearoyl-3-oleoyl-rac-  
732 glycerol). *Food Research International*. 2002;35:919–926. [https://doi.org/10.1016/S0963-](https://doi.org/10.1016/S0963-9969(02)00154-0)  
733 [9969\(02\)00154-0](https://doi.org/10.1016/S0963-9969(02)00154-0)

734

735 Talbot G. Properties of cocoa butter and vegetable fats. In: Beckett ST, Fowler MS, Ziegler GR  
736 editors. *Beckett's industrial chocolate manufacture and use*. 5th ed. Chichester: Wiley-  
737 Blackwell; 2017. p. 153–184. <https://doi.org/10.1002/9781118923597.ch7>

738

739 Timms RE. Phase behaviour of fats and their mixtures. *Progress in Lipid Research*. 1984;23:1–38.  
740 [https://doi.org/10.1016/0163-7827\(84\)90004-3](https://doi.org/10.1016/0163-7827(84)90004-3)

741

742 Timms RE. Confectionery fats handbook. Woodhead Publishing Limited; 2003

743

744 Watanabe S, Yoshikawa S, Arishima T, Sato K. Polymorphism and mixing phase behavior in ternary  
745 mixture systems of SOS-SSO-OSO: Formation of molecular compound crystals. *Journal of the*  
746 *American Oil Chemists' Society*. 2018;95: 447–460. <https://doi.org/10.1002/aocs.12054>

747

748 Watanabe S, Yoshikawa S, Sato K. Formation and properties of dark chocolate prepared using fat  
749 mixtures of cocoa butter and symmetric/asymmetric stearic-oleic mixed-acid triacylglycerols:  
750 Impact of molecular compound crystals, *Food Chemistry*. 2021;339:127808.  
751 <https://doi.org/10.1016/j.foodchem.2020.127808>

752

753 Wesdorp LH, van Meeteren J, de Jon S, Giessen R, Overbosch P, Grootcholten P, Liquid-multiple  
754 solid phase equilibria in fats: theory and experiments. In: Marangoni AG, Wesdorp LH, editors.  
755 *Structure and properties of fat crystal networks*. Volume 2. 2nd ed. Boca Raton: CRC Press; 2013.  
756 p. 241–418. <https://doi.org/10.1201/b12883>

757

758 Wijarnprecha K, West R, Rousseau D. Temperature-Dependent Mixing Behavior of Tristearin and  
759 1,2-Distearoyl-3-oleoyl-rac-glycerol (SSO). *Crystal Growth & Design*. 2023;23:4807–4814.  
760 <https://doi.org/10.1021/acs.cgd.2c01514>

761

762 Ye Y, Tan CY, Kim DA, Martini S. Application of high-intensity ultrasound to a zero-trans shortening  
763 during temperature cycling at different cooling rates. *Journal of the American Oil Chemists'*  
764 *Society*. 2014;91:1155–1169. <https://doi.org/10.1007/s11746-014-2458-6>

765

766 Yoshikawa S, Kida H, Sato K. Promotional effects of new types of additives on lipid crystallization.  
767 Journal of Oleo Science. 2014;63:333–345. <https://doi.org/10.5650/jos.ess13155>  
768

769 Yoshikawa S, Watanabe S, Yamamoto Y, Kaneko F, Sato K. Interactive Polymorphic Crystallization  
770 Behavior in Eutectic Triacylglycerol Mixtures Containing Molecular Compound Crystals. Crystal  
771 Growth & Design. 2022;22:1753–1763. <https://doi.org/10.1021/acs.cgd.1c01340>  
772

773 Zhang L, Ueno S, Miura S, Sato K. Binary Phase Behavior of 1,3-dipalmitoyl-2-oleoyl-*sn*-glycerol  
774 and 1,2-dioleoyl-3-palmitoyl-*rac*glycerol. Journal of the American Oil Chemists' Society.  
775 2007;84:219–227. <https://doi.org/10.1007/s11746-006-1034-0>  
776

777 Zhang L, Ueno S, Sato K, Adlof RO, List GR. Thermal and structural properties of binary mixtures of  
778 1,3-distearoyl-2-oleoyl-glycerol (SOS) and 1,2-dioleoyl-3-stearoyl-*sn*-glycerol (*sn*-OOS). Journal  
779 of Thermal Analyses and Calorimetry. 2009;98:105–111. [https://doi.org/10.1007/s10973-009-](https://doi.org/10.1007/s10973-009-0451-3)  
780 0451-3  
781

782 Zhang L, Ueno S, Sato K. Binary phase behavior of saturated-unsaturated mixed-acid triacylglycerols  
783 - A review. Journal of Oleo Science. 2018;67:679–687. <https://doi.org/10.5650/jos.ess17263>  
784

785 Zhang L, Wei KJ, Chen JC, Xiong M, Li X, Hondoh H, Ueno S. Effect of Cis–Trans Isomerization on  
786 the Crystallization Behavior of Triacylglycerols. Crystal Growth & Design. 2020;20:1655–1664.  
787 <https://doi.org/10.1021/acs.cgd.9b01406>